The ChvG–ChvI and NtrY–NtrX two-component systems coordinately regulate growth of *Caulobacter crescentus*

Benjamin J. Stein, Aretha Fiebig, Sean Crosson#

Department of Microbiology and Molecular Genetics, Michigan State University, East Lansing, MI, USA

#Correspondence: crosson4@msu.edu

Abstract

Two-component signaling systems (TCSs) regulate cellular homeostasis in response to changes in the environment. Typical TCSs comprise a sensor histidine kinase and a response regulator; the kinase senses environmental conditions and relays this information via phosphoryl transfer to its cognate response regulator, which controls gene expression. Bacteria often express many TCS gene pairs that control distinct physiological processes, but the regulatory connections between TCSs remain underexplored. We have identified regulatory links between the ChvG–ChvI (ChvGI) and NtrY–NtrX (NtrYX) TCSs, which control important and often overlapping processes in α-proteobacteria, including maintenance of the cell envelope. Deletion of *chvG* and *chvI* in *Caulobacter crescentus* limited growth in defined medium and a selection for genetic suppressors of this growth phenotype uncovered interactions among *chvGI*, *ntrYX*, and *ntrZ*. We found that NtrZ, a previously uncharacterized periplasmic protein, functions upstream of the NtrY sensor kinase. We observed significant overlap in the ChvI and NtrX transcriptional regulons, which provides support for the genetic connection between *ntrYX* and *chvGI*. Our analyses indicated that the growth defect of strains lacking ChvGI is determined by the phosphorylation state of NtrX and, to some extent, by the level of the TonB-dependent receptor ChvT. To explain the genetic interaction between these TCSs, we propose a model in which NtrZ functions in the periplasm to regulate the NtrY kinase, promoting phosphorylation of NtrX and modulating the regulatory overlap between NtrX and ChvI.

Importance

Two-component signaling systems (TCSs) enable bacteria to regulate gene expression in response to physiochemical changes in their environment. The ChvGI and NtrYX TCSs regulate diverse pathways associated with pathogenesis, growth, and cell-envelope function in many α-proteobacteria. We used *Caulobacter crescentus* as a model to investigate regulatory connections between ChvGI and NtrYX. Our work defined the ChvI transcriptional regulon in *C. crescentus* and uncovered significant overlap with the NtrX regulon. We revealed a genetic interaction between ChvGI and NtrYX, whereby modulation of NtrYX signaling affects the survival of cells lacking ChvGI. Finally, we identified NtrZ as a novel NtrY regulator. Our work establishes *C. crescentus* as an excellent model to investigate multi-level regulatory connections between ChvGI and NtrYX in α-proteobacteria.

Introduction

Bacteria employ two-component signaling systems (TCSs) to respond to environmental cues and maintain cellular homeostasis (1). TCS sensory modules consist of two core components: a sensory histidine kinase (HK) and a response regulator (RR). In response to signal(s), the HK undergoes autophosphorylation on a conserved histidine residue, and then passes the phosphoryl group to a conserved aspartate on the receiver (REC) domain of the RR (1). RR phosphorylation generally alters the activity of effector domains that change gene expression. TCSs are modular, with the output of a particular RR varying between different organisms (2-5). Thus, TCSs that regulate host interactions in pathogens and symbionts are often employed by related free-living organisms to respond to similar features in the environment (2, 6-8).

Although typical TCSs rely on a single HK and RR pair, many systems incorporate additional proteins, such as activators or inhibitors, to form more complex signaling networks (9-17). Historically, most TCSs have been considered to be insular systems, but in many bacteria, crosstalk between HKs and RRs may integrate multiple environmental cues (9, 11, 14, 18-20). Even when HK and RR pairs are well insulated, TCSs can interact at the transcriptional level (20, 21). For example, one TCS may regulate the expression of other TCS genes, or multiple TCSs may influence transcription of the same downstream gene (22-24).

ChvG–ChvI (ChvGI) and NtrY–NtrX (NtrYX) are conserved α-proteobacterial TCSs that often regulate similar physiological processes, raising the possibility that they may work together in a coordinated fashion (25, 26). The ChvG HK and ChvI RR were originally identified as pleiotropic regulators in the plant pathogen *Agrobacterium tumefaciens*, affecting virulence, detergent tolerance, and pH sensitivity (8, 27). Subsequent work has linked ChvGI to host interaction, cell motility, acid sensing, and exopolysaccharide production in a variety of α-proteobacteria (6, 7, 28-32). In most characterized systems, the periplasmic protein ExoR binds to ChvG and inhibits its kinase activity (15, 16, 33). Acidic pH activates the ChvGI system by triggering rapid proteolysis of ExoR (34). However, not all organisms with ChvGI, including *Caulobacter crescentus*, contain ExoR. Therefore, these bacteria must regulate ChvG kinase activity by a different mechanism.

Like ChvGI, NtrYX (consisting of the NtrY HK and NtrX RR) is conserved in many α-proteobacteria, including multiple pathogens and symbionts (35-39). Although early studies primarily showed that NtrYX regulates nitrogen metabolism, recent work suggests that, in certain α-proteobacteria, it also affects exopolysaccharide biosynthesis, cell motility, and cell envelope composition (25, 35, 39, 40-44). These processes are also regulated by ChvGI, suggesting that ChvGI and NtrYX might act coordinately. However, to date, no work has identified a substantial genetic interaction between these TCSs (25, 26).

C. crescentus, a free-living α-proteobacterium found in freshwater and soil environments, contains homologs of both ChvGI and NtrYX (45, 46). *C. crescentus* ChvGI

activates transcription of the small regulatory RNA *chvR*, which post-transcriptionally represses the TonB-dependent receptor gene *chvT* (6). In addition, examination of reporters of *chvR* transcription indicated that ChvGI is activated by growth in defined medium, acidic pH, DNA damage, growth at stationary phase, and cell envelope stress (6, 47). However, aside from *chvR*, genes regulated by ChvGI have not been identified. *C. crescentus* NtrYX is less well-characterized than ChvGI, but a recent study established that NtrX is phosphorylated in stationary phase in defined medium, as a result of acidification (48). In addition, NtrX appears to play a core role in regulating *C. crescentus* physiology, as *ntrX* is essential for growth in complex medium and *ΔntrX* cells grow more slowly than wild-type (WT) cells in defined medium (49).

In this study, we initially took a reverse genetics approach to characterize the role of ChvGI in regulating *C. crescentus* physiology. Deletion of *chvG* and *chvI* caused a distinctive growth defect in defined medium. By exploiting this defect, we identified striking genetic interactions between *chvGI* and *ntrY*, *ntrX*, and *ntrZ* (an uncharacterized gene predicted to encode a regulator of NtrY). Epistasis analysis revealed that the presence of NtrX, likely in its unphosphorylated form, is detrimental to cells lacking *chvG* or *chvI*. Moreover, we defined the ChvI transcriptional regulon and discovered that it overlaps significantly with genes regulated by NtrX. We conclude that ChvGI and NtrYX interact at multiple transcriptional levels, working both in concert and in opposition to regulate growth in defined medium.

Results

Loss of the ChvGI system limits growth in defined medium

To investigate the physiological relevance of ChvGI in *C. crescentus*, we generated strains with in-frame deletions of *chvG* or *chvI* and examined their growth. The deletion strains grew normally in complex medium (peptone-yeast extract, PYE), but they displayed a distinctive growth defect in defined medium (M2 minimal salts medium with xylose as carbon source, M2X) (Fig. 1A, 1B and Fig. S1). Although overnight cultures for each strain grew to similar densities in M2X, upon dilution strains lacking *chvG* or *chvI* exhibited reduced growth capacity, reaching a terminal density of only OD_{660} ~ 0.1 (Fig. 1A). This lower cell density correlated with fewer colony-forming units (CFUs) (Fig. 1B). Ectopic overexpression of *chvG* or *chvI* fully rescued growth of *ΔchvG* or *ΔchvI* strains, respectively, under these conditions (Fig. 1A, 1B).

To evaluate if the growth defect correlated with cell division capacity in defined medium, we resuspended cells in M2X from PYE agar plates and diluted cultures to several low starting densities. *ΔchvI* EV cultures started at OD_{660} = 0.001 and 0.0001 saturated at similar CFU values (~10^7 CFU/mL) that were significantly lower than those of *ΔchvI chvI++* cultures (~10^9 CFU/mL) (Fig. 1C). Thus, *ΔchvI* mutants are not limited in the number of times they can divide in M2X medium, but rather reach a defined carrying capacity. Starting *ΔchvI* cultures at high densities (OD_{600} = 0.05 and 0.1) led to a greater final density (~10^9 CFU/mL), indicating that starting density determines

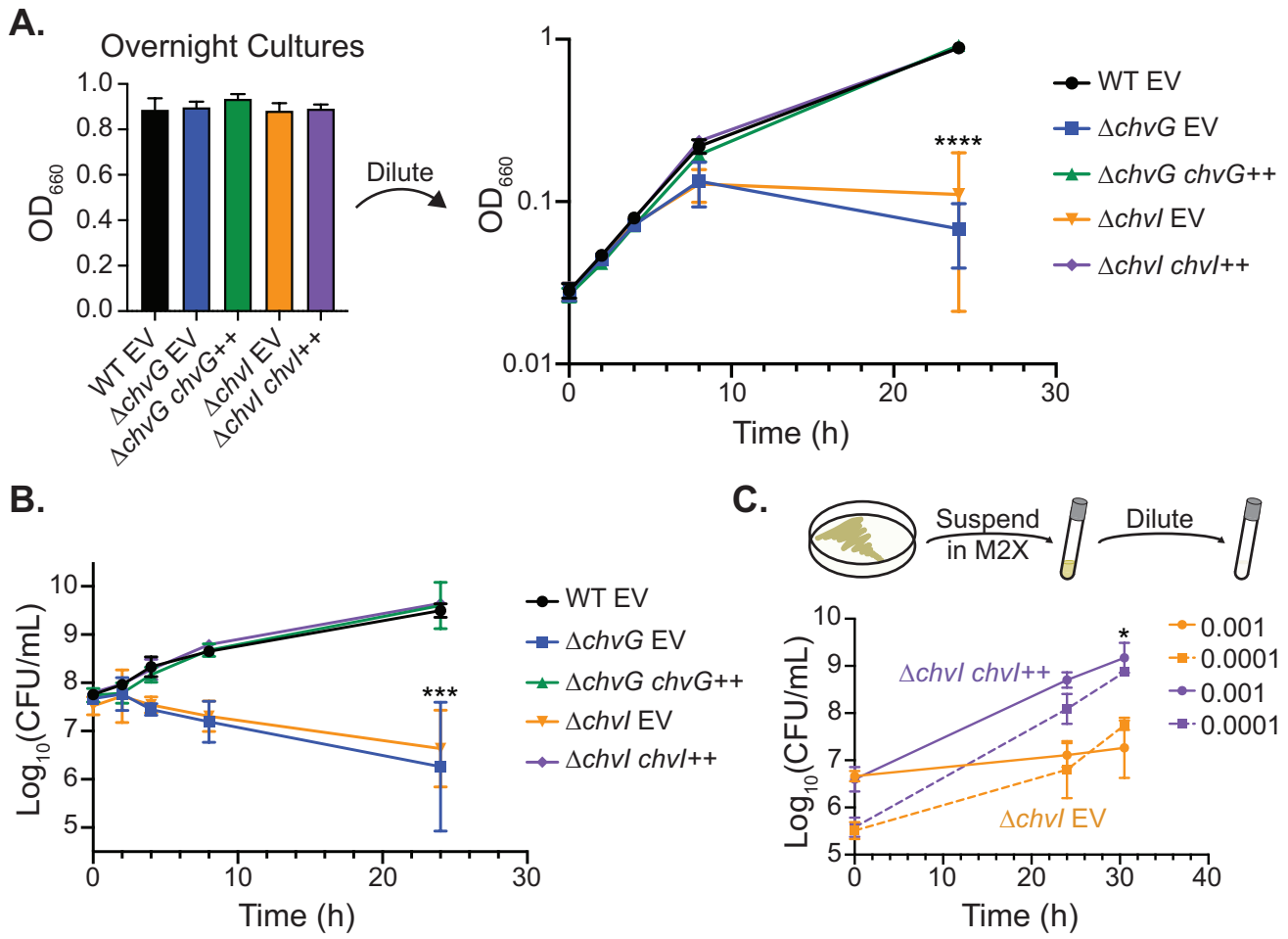

Figure 1: Loss of *chvG* or *chvI* limits culture density in defined M2X medium.
A. Growth curves, measured by optical density (OD_{660}), of WT, *ΔchvG*, and *ΔchvI* strains bearing empty vector (EV) or genetic rescue plasmid (++) integrated at the xylose locus. Primary M2X cultures, inoculated from PYE plates, all grow to high density (left). However, upon back-dilution to $OD_{660} = 0.025$, *ΔchvG* and *ΔchvI* EV strains saturate at a significantly lower OD (right). Points represent averages of three biological replicates ± SD. **** = $p < 0.0001$, one-way ANOVA followed by Dunnett's post-test comparison to WT EV at 24 h. **B.** Growth curves, measured by CFU, corresponding to the cultures in A. Points represent averages of three biological replicates ± SD. **** = $p < 0.0001$, *** = $p < 0.0005$, one-way ANOVA followed by Dunnett's post-test comparison to WT EV at 24 h. **C.** Growth of cultures inoculated from PYE agar plates at different starting densities, measured by CFU. *ΔchvI* cells carrying empty vector (EV) or genetic rescue plasmid (++) were suspended in M2X medium and immediately diluted to $OD_{660} = 0.001$ or 0.0001. Points represent averages of three biological replicates ± SD. * = $p < 0.05$, one-way ANOVA followed by Dunnett's post-test comparison to *ΔchvI* EV, 10^{-4} dilution at 30.5 h.

whether primary overnight cultures reach high density at saturation (Fig. S2A).

Washing *ΔchvI* cells once or twice with M2X before dilution had no effect on the number of CFUs at 30.5 h, suggesting that trace contaminating PYE components do not contribute to growth in M2X (Fig. S2B). Moreover, cell density alone did not determine the ability of *ΔchvI* cultures to grow in M2X, as denser back-dilutions from *ΔchvI* overnight cultures did not reach higher viable cell counts (Fig. S2C). Together, our results suggest that the growth capacity of *ΔchvI* or *ΔchvG* cells in M2X medium reflects a combination of the time

since resuspension from PYE plates and growth phase.

ChvI phosphorylation is critical for growth in defined medium

Given the similarity between the phenotypes displayed by *ΔchvI* and *ΔchvG* strains, we predicted that phosphorylation of ChvI might be important for growth in M2X medium. To test this hypothesis, we generated

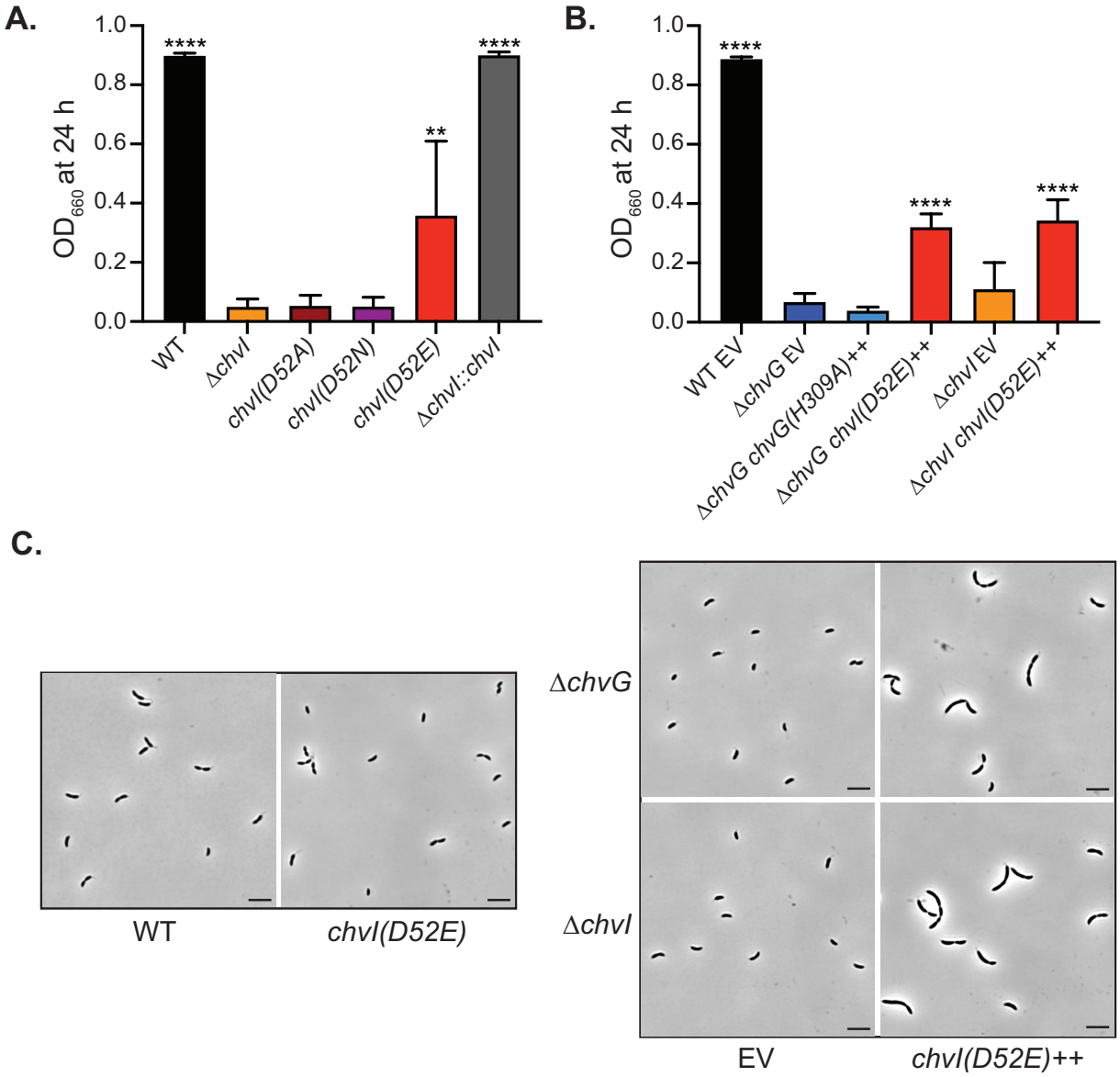

Figure 2: The *chvI(D52E)* allele is active and induces filamentation in M2X medium when overexpressed.
A. Optical density (OD_{660}) of cultures 24 h after back-dilution to $OD_{660} = 0.025$ in M2X medium (Average ± SD, $N \geq 4$). *chvI* mutant strains were generated by restoring the *ΔchvI* allele with point-mutant alleles. Similarly, restored WT (*ΔchvI*::*chvI*) was generated by replacement of the *ΔchvI* locus with WT *chvI* . * = $p < 0.05$, ** = $p < 0.01$, one-way ANOVA followed by Dunnett's post-test comparison to *ΔchvI*. **B.** Optical density (OD_{660}) of strains carrying empty vector (EV) or overexpression plasmids (++) 24 h after back-dilution to $OD_{660} = 0.025$ in M2X medium (average ± SD, $N = 3$). **** = $p <$ 0.0001, one-way ANOVA followed by Dunnett's post-test comparison to *ΔchvG* EV. **C.** Phase-contrast micrographs of primary overnight cultures grown in M2X medium. On the right, *ΔchvI* and *ΔchvG* strains carry empty vector (EV) or overexpression plasmids (++). Scale bars, 5 μm.

strains harboring *chvI* alleles encoding changes to the conserved sites of phosphorylation (D52A, D52N, and D52E). Growth of strains carrying the non-phosphorylatable alleles *chvI(D52A)* and *chvI(D52N)* was similar to *ΔchvI* cells in M2X (Fig. 2A and Fig. S3A). By contrast, *chvI(D52E)* cultures reached higher densities than *ΔchvI* cultures, suggesting that ChvI(D52E) is active, albeit not to the same level as WT ChvI (Fig. 2A and Fig. S3A). Substitutions of the phosphorylatable aspartate with glutamate often act as phosphomimetic mutations and constitutively activate RRs (50-53). Thus, this result supports a critical role for ChvI phosphorylation during growth in M2X medium.

To further examine the importance of ChvI phosphorylation, we overexpressed *chvG* and *chvI* alleles in knockout backgrounds. Although overexpression of *chvG* rescued growth of *ΔchvG* cells (Fig 1B), overexpression of *chvG(H309A),* a catalytic-histidine mutant, did not, indicating that phosphorylation of ChvG, and by extension ChvI, is important for growth in M2X medium (Fig. 2B). Overexpression of *chvI(D52E)* only partially rescued growth of *ΔchvI* and *ΔchvG* strains in M2X and these strains behaved similarly to the strain encoding *chvI(D52E)* at the native locus (Fig. 2A, 2B and Fig. S3B). However, in contrast to native expression of *chvI(D52E)*, overexpression of

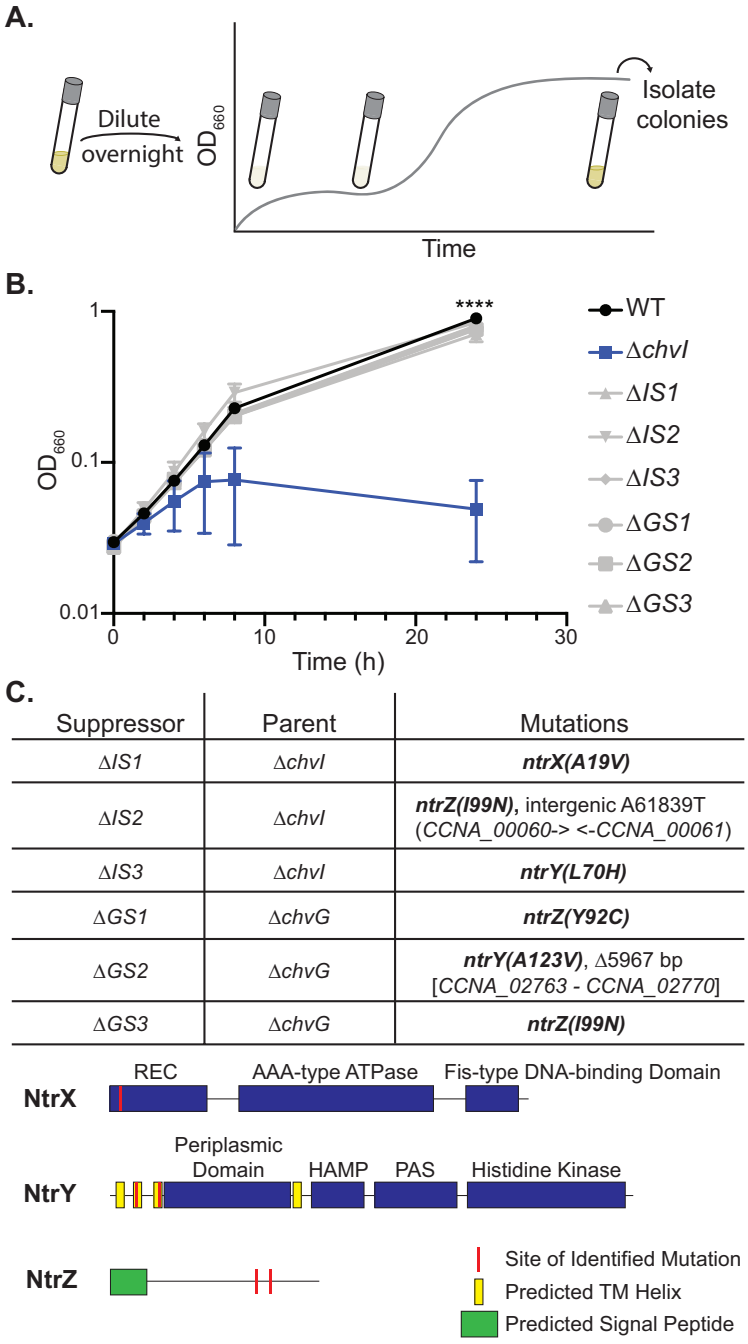

Suppressor	Parent	Mutations
ΔIS1	ΔchvI	***ntrX(A19V)***
ΔIS2	ΔchvI	***ntrZ(I99N)***, intergenic A61839T (*CCNA_00060-> <-CCNA_00061*)
ΔIS3	ΔchvI	***ntrY(L70H)***
ΔGS1	ΔchvG	***ntrZ(Y92C)***
ΔGS2	ΔchvG	***ntrY(A123V)***, Δ5967 bp [*CCNA_02763 - CCNA_02770*]
ΔGS3	ΔchvG	***ntrZ(I99N)***

Figure 3: Mutations in the NtrYX TCS and a gene of unknown function suppress the growth defect of *ΔchvG* and *ΔchvI* cells in M2X medium.

A. Schematic representation of the suppressor selection protocol. Primary overnight cultures in M2X medium were back-diluted to OD_{660} = 0.025 and grown until cultures grew to high turbidity. Single colonies were isolated for confirmation and sequencing. **B.** Growth curves, measured by optical density (OD_{660}), of WT, *ΔchvI*, and suppressor strains isolated from either the *ΔchvI* strain (*ΔIS#*) or the *ΔchvG* strain (*ΔGS#*) upon back-dilution in M2X medium. Points represent averages of three biological replicates ± SD. **** = $p < 0.0001$, one-way ANOVA followed by Dunnett's post-test comparison to *ΔchvI* at 24 h. **C.** Whole-genome sequencing results of each suppressor strain. The suppressor strain, parental strain, and identified polymorphism(s) are indicated. Mutations in *ntrY*, *ntrX*, and *ntrZ* (*CCNA_03863*) are in bold. Domain structures of NtrY, NtrX, and NtrZ are diagramed with domains in blue, signal peptides in green, transmembrane helices in yellow, and identified mutations in red.

this allele resulted in cell filamentation in M2X, consistent with a cell division defect (Fig. 2C and Fig. S3C). Thus, overexpression of phosphomimetic *chvI(D52E)* appears to interfere with cell division and, as a result, only partially rescues growth in M2X medium.

Mutations in ntrY, ntrX, and a gene of unknown function, rescue the growth defect of ΔchvI and ΔchvG strains

To better understand why ChvGI is critical for growth in defined medium, we employed a selection strategy to isolate second-site mutations that alleviate the growth defect of *ΔchvG* and *ΔchvI* cells. *ΔchvG* and *ΔchvI* M2X-overnight cultures were back-diluted and grown until they reached high density, presumably due to proliferation of suppressor strains (Fig. 3A). We then isolated single colonies with WT-like growth in M2X and used whole-genome sequencing to identify any acquired mutations (Fig. 3B).

In multiple independent strains, we identified nonsynonymous substitutions in the genes encoding the HK NtrY and its cognate RR NtrX (Fig. 3C). The *ntrY* mutations (L70H and A123V) are located in predicted transmembrane helices, which are involved in transmitting information from periplasmic sensing domains to the kinase domain (Fig. 3C) (54-56). We identified only one *ntrX* allele, A19V, which lies in helix 1 (α1) of the receiver domain (Fig. 3C). α1 is involved in the interaction interface between the HK DHp domain and the RR REC domain (57, 58). We also note that the *ntrX(A19V)* strain was isolated on PYE plates and appeared to grow normally in M2X, suggesting that this is not a complete loss-of-function allele (49).

In addition to mutations in *ntrY* and *ntrX*, we identified three clones with nonsynonymous substitutions in a gene encoding a putative periplasmic protein of unknown function (*CCNA_03863*, hereafter referred to as *ntrZ*) (Fig. 3C). The mutations identified (Y92C and I99N) are both located in the putative periplasmic domain (Fig. 3C). Therefore, modulation of NtrYX and a gene of unknown function can affect the growth of *ΔchvI* and *ΔchvG* cells in M2X medium.

Overexpression or deletion of ntrX actuates the ΔchvI growth phenotype

Several studies have noted similar phenotypes in *chvGI* and *ntrYX* mutants (25, 26, 41); however, to our knowledge none have established a genetic link between these TCSs. To better understand the connections between ChvGI and NtrYX in *C. crescentus*, we first characterized the genetic relationship between *chvI* and *ntrX*. Replacement of *ntrX* with the *ntrX(A19V)* allele indeed restored growth of *ΔchvI* cells in M2X (Fig. 4A), ruling out any undetected background mutations as causal for the suppressor phenotype. However, overexpression of *ntrX(A19V)* in the presence of the native *ntrX* allele did not rescue growth of *ΔchvI* cells (Fig. 4A). This result indicates that the *ntrX(A19V)* allele is recessive, and suggests that the presence of WT NtrX is problematic in *ΔchvI* cells.

To examine this notion further, we tested the effect of deleting *ntrX* in the *ΔchvI* strain. *ΔntrX* cells had a slight growth defect in M2X, but were clearly distinct from *ΔchvI* cells (Fig. 4B). Deletion of *ntrX* in strains lacking *chvI*

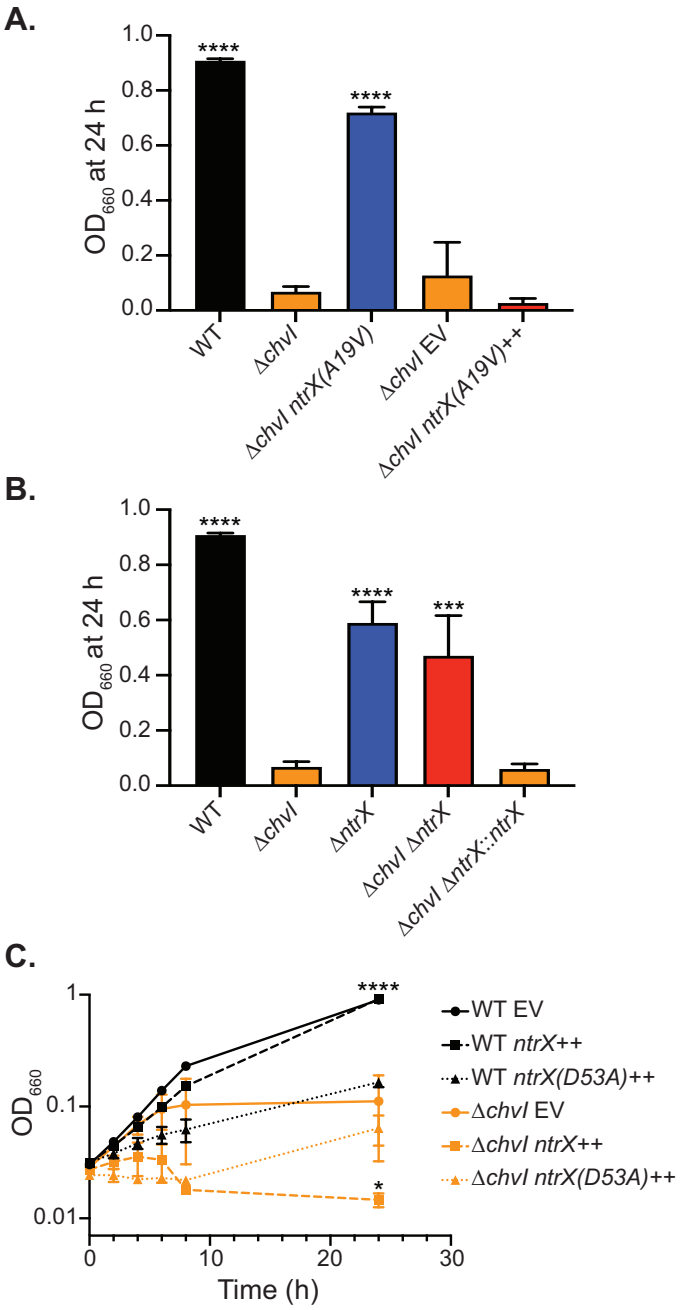

Figure 4: Non-phosphorylatable NtrX limits growth of cells in M2X medium.

A. Optical density (OD_{660}) of cultures 24 h after back-dilution to OD_{660} = 0.025 in M2X medium (average ± SD, $N = 3$). The *ntrX(A19V)* allele was introduced by allele replacement for comparison with WT and *ΔchvI* or by overexpression (++) for comparison with an empty vector (EV) strain. **** = $p < 0.0001$, one-way ANOVA followed by Dunnett's post-test comparison to *ΔchvI*. **B.** Optical density (OD_{660}) of cultures 24 h after back-dilution to OD_{660} = 0.025 in M2X medium (average ± SD, $N = 3$). Restored *ΔchvI* (*ΔchvI ΔntrX*::*ntrX*) was generated by knocking *ntrX* into the native *ntrX* locus in *ΔchvI ΔntrX* cells. *** = $p < 0.0005$, **** = $p < 0.0001$, one-way ANOVA followed by Dunnett's post-test comparison to *ΔchvI*. **C.** Growth curves, measured by optical density (OD_{660}), of strains upon back-dilution in M2X medium. WT and *ΔchvI* strains bear empty vector (EV) or *ntrX* overexpression vectors (++). Points represent averages of three biological replicates ± SD. * = $p < 0.05$, **** = $p < 0.0001$, one-way ANOVA followed by Dunnett's post-test comparison to *ΔchvI* EV at 24 h.

rescued growth to levels seen for *ΔntrX* cells, indicating that the presence of *ntrX* is indeed detrimental to *ΔchvI* cells (Fig. 4B). This suppression was not due to a second-site mutation, as restoration of the *ntrX* locus (*ΔchvI ΔntrX*::*ntrX)* restored the growth defect in M2X medium (Fig. 4B).

Given that the presence of *ntrX* limits growth of *ΔchvI* cells in M2X, we next tested whether overexpression of *ntrX* affects growth of WT cells. Overexpression of *ntrX* only moderately slowed growth of WT cells. However, overexpression of the non-phosphorylatable *ntrX(D53A)* allele dramatically impaired the growth of WT cells in M2X, similar to the defect observed in *ΔchvI* cells (Fig. 4C). Overexpression of either *ntrX* or *ntrX(D53A)* exacerbated the growth defect of *ΔchvI* cells (Fig. 4C). In addition, cells lacking the NtrY HK were more sensitive to *ntrX* overexpression than WT cells in M2X (Fig. S4A, S4B). Together these results support a model in which unphosphorylated NtrX limits growth capacity in M2X medium, especially in *ΔchvI* cells.

NtrZ is a predicted periplasmic protein that functions upstream of the NtrY kinase

We next examined the nature of the *ntrY* and *ntrZ* suppressor mutations. Overexpression of the *ntrY* and *ntrZ* alleles identified in our

suppressor strains restored growth of *ΔchvI* cells in M2X (Fig. 5A). In addition, overexpression of WT *ntrY*, but not WT *ntrZ*, also significantly suppressed the *ΔchvI* growth defect (Fig. 5A). We conclude that the *ntrY* and *ntrZ* mutations are dominant, likely gain-of-function, alleles. As deletion of *ntrX* rescued the growth of *ΔchvI* cells, overexpression of *ntrY* or *ntrZ* mutant alleles likely promotes phosphorylation and/or sequestration of NtrX.

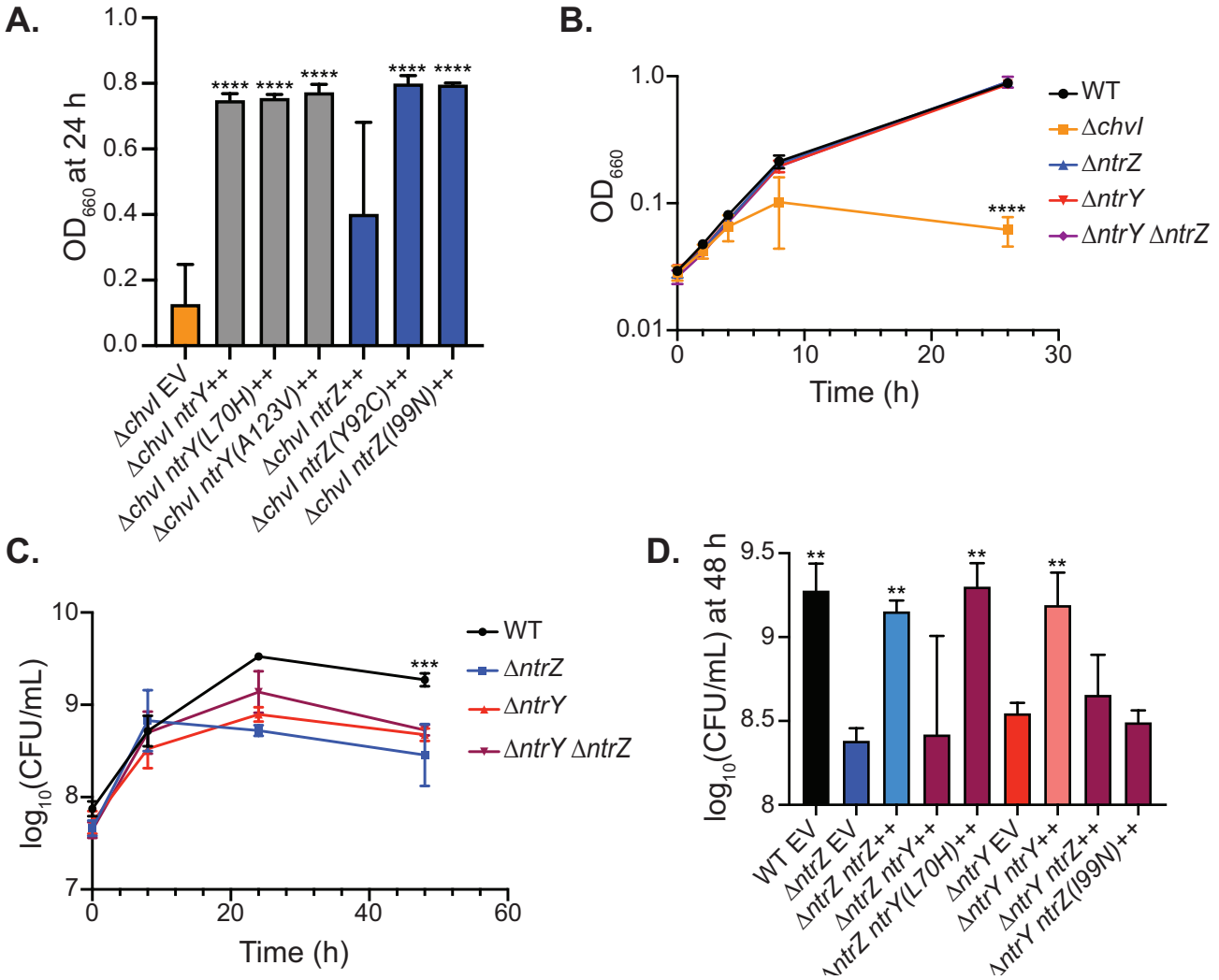

Figure 5: NtrZ functions upstream of NtrY to promote survival during stationary phase in M2X medium. **A.** Optical density (OD_{660}) of strains bearing empty vector (EV) or *ntrZ* and *ntrY* overexpression vectors (++) 24 h after back-dilution to OD_{660} = 0.025 in M2X medium (average ± SD, $N = 3$). **** = $p < 0.0001$, one-way ANOVA followed by Dunnett's post-test comparison to *ΔchvI* EV. **B.** Growth curves, measured by optical density (OD_{660}), of WT and knockout strains upon back-dilution in M2X medium. Points are averages of three biological replicates ± SD. **** = $p < 0.0001$, one-way ANOVA followed by Dunnett's post-test comparison to WT at 24 h. **C.** Growth curves, measured by CFU, for WT and mutant strains grown in M2X medium. Points are averages of three biological replicates ± SD. *** = $p = 0.0005$, one-way ANOVA followed by Dunnett's post-test comparison to *ΔntrZ* at 48 h. **D.** Cell density, measured by CFU, for *ΔntrZ* and *ΔntrY* strains bearing empty vector (EV) or overexpression vectors (++) at 48 h growth in M2X medium. Points are averages of three biological replicates ± SD. ** = $p < 0.01$, one-way ANOVA followed by Dunnett's post-test comparison to *ΔntrZ* EV at 48 h.

We attempted, but failed, to construct *ΔchvI ΔntrY* and *ΔchvI ΔntrZ* double-mutant strains, suggesting that loss of either *ntrY* or *ntrZ* may result in synthetic lethality when combined with the loss of *chvI*. This inability to isolate either double mutant also hinted that NtrY and NtrZ might function in the same pathway. To test this possibility, we evaluated the phenotype of *ntrY* and *ntrZ* deletions in M2X medium. However, the growth of both single deletions and the Δ*ntrY ΔntrZ* double deletion was indistinguishable from WT, thus preventing epistasis analysis (Fig. 5B).

Phosphorylation of NtrX is likely important for stationary phase survival (48), and thus, we hypothesized that deletion of the *ntrY* HK, and perhaps also *ntrZ*, might lead to a stationary-phase defect. Indeed, we observed significantly lower CFUs in both *ΔntrY* and *ΔntrZ* cultures compared to WT cultures after 48 h of growth in M2X (Fig 5C). Notably, *ΔntrY ΔntrZ* cultures behaved similarly to the single mutants, suggesting that NtrY and NtrZ indeed function in the same pathway.

To place *ntrY* and *ntrZ* relative to one another, we evaluated the ability of *ntrY* and *ntrZ* alleles to rescue stationary-phase survival in the deletion strains. Both *ΔntrY* and Δ*ntrZ* cells were fully rescued by ectopic overexpression of each respective WT allele (Fig. 5D). Overexpression of *ntrY(L70H)*, but not *ntrY*, also fully rescued the phenotype of *ΔntrZ* cells (Fig. 5D). By contrast, neither WT *ntrZ* nor *ntrZ(I99N)* rescued *ΔntrY* cells (Fig. 5D). These data provide evidence that NtrZ functions upstream of NtrY, potentially as a kinase activator and/or phosphatase inhibitor.

Our characterization of the *ntrY*, *ntrX*, and *ntrZ* mutants suggested that phosphorylation of NtrX may rescue the growth of *ΔchvI* or *ΔchvG* cells. NtrX is phosphorylated under acidic conditions, such as those encountered during stationary phase in M2X medium (48). Therefore, we tested whether the pH of M2X affected the growth of *ΔchvI* cultures. For both WT and *ΔchvI* strains, primary overnight cultures diluted in M2X at pH 7.0 reached similar CFUs at 8 h as those diluted in standard M2X (pH 7.2) (Fig. 1B, S4C). WT cultures were relatively unaffected by growth in M2X at pH 6.0, but had significantly fewer CFUs in M2X pH 5.5 vs. pH 7.0 (Fig. S4C). By contrast, *ΔchvI* cells were markedly less fit in M2X pH 6.0 than at pH 7.0, and displayed an intermediate growth yield at pH 5.5 relative to M2X at either pH 6.0 or pH 7.0 (Fig. S4C). These results are consistent with the suppression of *ΔchvI* growth defects by NtrX phosphorylation and a role for ChvGI in acid-stress responses (6).

ChvI and NtrX regulate transcription of an overlapping set of genes

Although ChvGI is known to regulate the expression of *chvR*, the complete ChvI transcriptional regulon is not known. To examine the regulatory link between *ntrX* and *chvI* in greater detail, we performed an RNA-seq experiment to comprehensively define ChvI-dependent gene regulation. As *ΔchvI* cells grow poorly in M2X medium, we exploited overexpression of the phosphomimetic *chvI(D52E)* allele to assess ChvI-dependent transcription in PYE medium. Excluding the internal *chvI* control, we identified 162 genes with > 1.5 fold-change in *ΔchvI chvI(D52E)++*

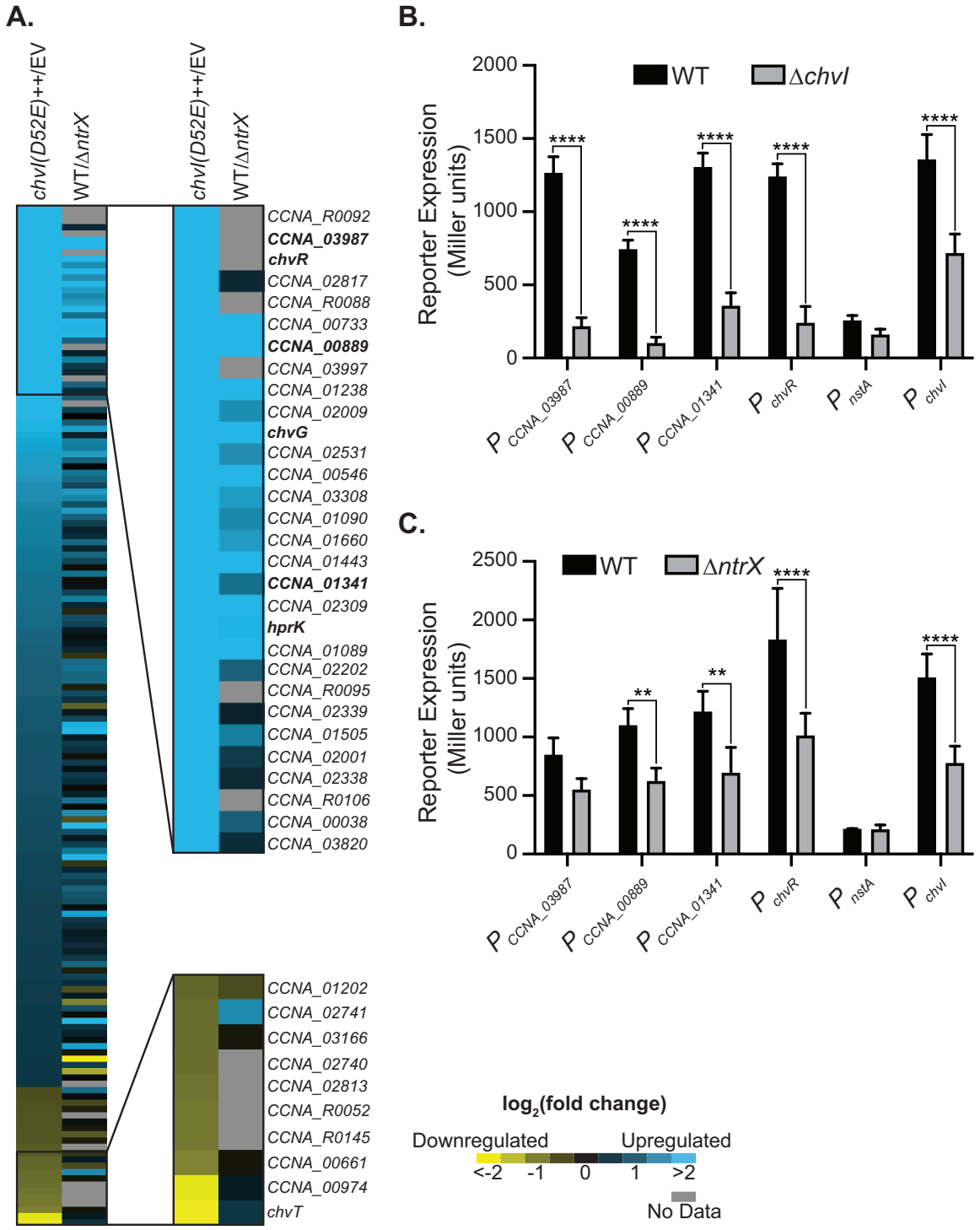

Figure 6: The ChvI and NtrX regulons overlap significantly.
A. Heat map of $\log_2$(fold change) for genes in the ChvI regulon (fold Change > 1.5, FDR *p*-value < 0.05) defined by RNA-seq (*ΔchvI chvI(D52E)*++ vs. *ΔchvI* EV). Log_2(fold change) is also shown for a microarray dataset comparing RNA levels in WT and *ΔntrX* cells (49); grey cells indicate no data. The genes most strongly regulated in the ChvI regulon are annotated. **B.** *lacZ* transcriptional reporter activity for a subset of genes in the ChvI regulon in WT and *ΔchvI* strains in M2X medium (average ± SD, $N = 3$). **** = $p < 0.0001$, one-way ANOVA followed by Šídák's post-test comparison for indicated pairs. **C.** *lacZ* transcriptional reporter activity for the same genes as in B in WT and *ΔntrX* strains in M2X medium (average ± SD, $N = 4$). ** = $p < 0.01$, **** = $p < 0.0001$, one-way ANOVA followed by Šídák's post-test comparison for indicated pairs.

cells compared to *ΔchvI* EV cells (Fig. 6A and Table S1). Of those, 140 were upregulated and 22 were downregulated, indicating that ChvI primarily serves as a transcriptional activator. Consistent with previous work, *chvR* was upregulated while *chvT* was downregulated by overexpression of *chvI(D52E)* (6, 47). In addition, expression of both *chvG* and *hprK* was enhanced in cells expressing *chvI(D52E)*, pointing to positive autoregulation of the *chvIG-hprK* operon. We also observed regulation of multiple genes involved in envelope maintenance, metabolism, protein quality control, and transport (Fig. S5A). ChvI-dependent genes included multiple genes encoding proteases/peptidases (*CCNA_01341*, *CCNA_02846*, *CCNA_01955*, *CCNA_02721*, *mmpA*, *CCNA_02594*, *CCNA_01121*, *CCNA_01202*), peptidyl-prolyl and disulfide isomerases (*CCNA_02889*, *CCNA_01654*, *CCNA_01759*, *CCNA_01653*, *CCNA_00378, CCNA_00379*), members of the β-barrel assembly machine (BAM) complex (*bamA*, *bamB*, *bamD*, *bamE*, *bamF*), members of the Tol–Pal complex (*tolB*, *ybgF*, *tolQ*), and lipopolysaccharide biosynthesis genes (*CCNA_01497*, *CCNA_03454*, *CCNA_01496*, *lpxC*). Moreover, nearly 40% of ChvI regulon genes encoded hypothetical proteins or proteins of unknown function (Fig. S5A). MEME analysis of the top 35 upregulated operons identified a putative ChvI binding motif, with GCC direct repeats 11-nt apart, that closely resembles the recently characterized binding motif of *Sinorhizobium meliloti* ChvI (Fig. S5B) (5).

As our regulon was defined by overexpression of a phosphomimetic ChvI mutant, we sought to validate our dataset under more physiological conditions. We constructed transcriptional β-galactosidase reporters for six selected regulon genes, from *nstA* (2-fold activation) to *CCNA_03987* (128-fold activation). Strains carrying these transcriptional reporters were initially grown in PYE medium, followed by back-dilution and 4 h of growth in M2X medium. Consistent with previous reports, the reporter for the *chvR* promoter (P_{chvR}) was expressed in M2X in a *chvI*-dependent manner (Fig. 6B) (6, 47). The remaining reporters, apart from P_{nstA}, which was expressed at low levels, also exhibited clear *chvI* dependence, supporting our RNA-seq results (Fig. 6B). Unlike the other reporters, P_{chvI} was only 2-fold lower in *ΔchvI* cells compared to WT cells, indicating that additional factors promote expression of the *chvIG-hprK* operon.

We next compared our ChvI regulon with a previously published NtrX regulon that was determined using DNA microarrays (49). This experiment measured relative gene expression between *C. crescentus* WT (strain NA1000) and *ΔntrX* cells during exponential growth in M2G medium, a condition where NtrX is expected to be largely unphosphorylated (48, 49). Surprisingly, a large fraction of the genes regulated by ChvI were also represented in the genes regulated by NtrX (Fig. 6A). That is, many of the genes upregulated by ChvI also appeared to be upregulated by NtrX (and likewise for downregulated genes). Using cutoffs of 1.5 fold-change for the ChvI RNA-seq data and 2.5 fold-change for the NtrX microarray data, we established that the ChvI regulon is significantly enriched for NtrX-dependent genes (6.31-fold enrichment, *p*-value = 8.99×10^{-19}, hypergeometric test). To confirm this overlap, we evaluated the effect of deleting *ntrX* on our ChvI regulon reporters. Strains carrying the

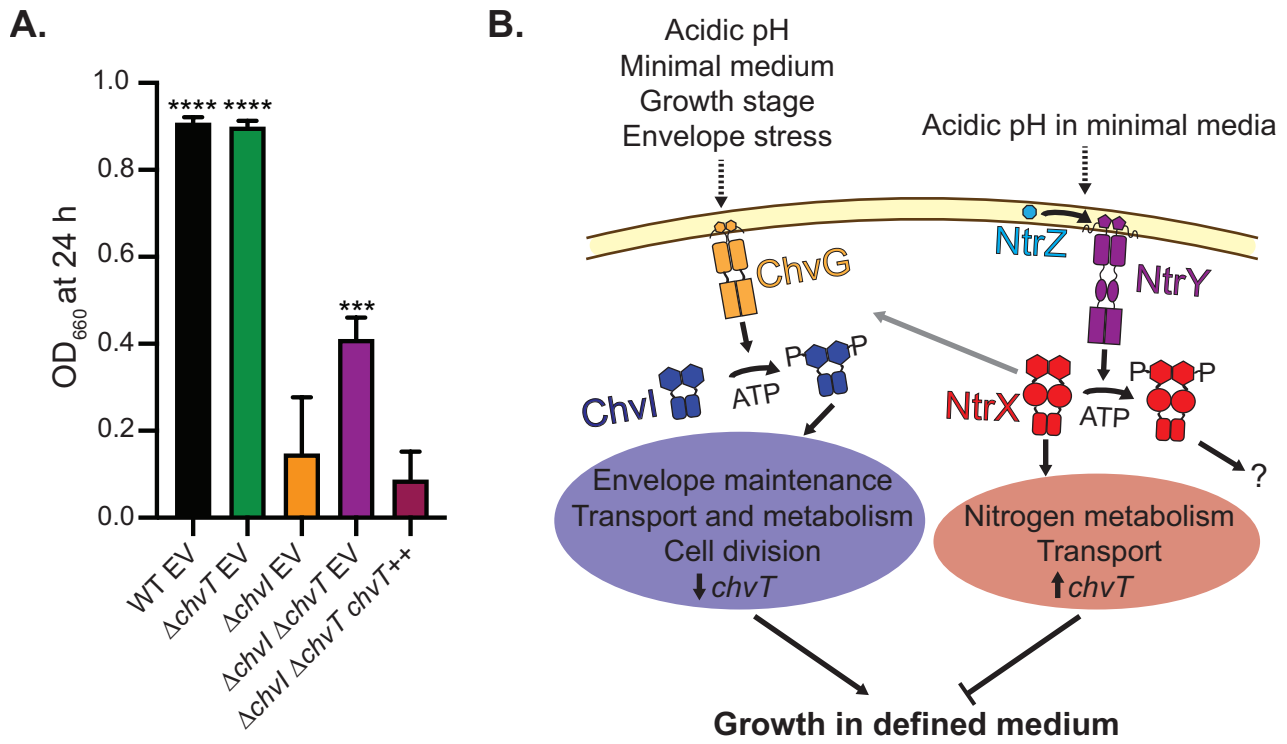

Figure 7: Deletion of *chvT* partially restores growth of *ΔchvI* cells in M2X medium.
A. Optical density (OD_{660}) of WT, ΔchvT, and *ΔchvI ΔchvT* strains, with empty vector (EV) or *chvT* overexpression vector (++), 24 h after back-dilution to $OD_{660} = 0.025$ in M2X medium (average ± SD, $N = 4$). *** = $p < 0.0005$, **** = $p < 0.0001$, one-way ANOVA followed by Dunnett's post-test comparison to *ΔchvI* EV. **B.** Proposed model for the regulatory interactions between ChvGI and NtrYX. ChvG (orange) is activated by a variety of cellular conditions (dashed arrow) and phosphorylates ChvI (blue). Phosphorylated ChvI regulates genes involved in envelope maintenance, transport, metabolism, and cell division (blue oval). In addition, ChvI represses expression of *chvT*. NtrY (purple) is activated under acidic conditions in defined medium (dashed arrow), potentially by NtrZ, and phosphorylates NtrX (red). Unphosphorylated NtrX regulates much of the ChvI regulon, likely via upregulation of the *chvIG-hprK* operon (grey arrow). In addition, unphosphorylated NtrX upregulates *chvT* and regulates expression of genes involved in nitrogen metabolism and transport (red oval). Phosphorylated ChvI and unphosphorylated NtrX oppose each other in regulating growth in defined medium, partially via differential regulation of *chvT*. The transcriptional role of phosphorylated NtrX (question mark) is not yet known.

transcriptional reporters were grown to log phase (OD_{660} ~ 0.1–0.2) in M2X medium before assaying β-galactosidase activity. Four of the six reporters exhibited *ntrX* dependence, including two genes (*CCNA_00889* and *chvR*) not evaluated in the NtrX microarray experiment (Fig. 6C). We note that transcription from the *chvI* promoter (P_{chvI}) was activated by both *ntrX* and *chvI*, raising the possibility that NtrX may indirectly affect ChvI-dependent genes via upregulation of *chvIG-hprK*.

Given the oppositional nature of ChvI and NtrX during growth in M2X medium, we were surprised to see such a high degree of similarity in the genes they regulate. However, a small subset of genes exhibited opposite regulation by ChvI and NtrX, which might therefore account for suppression of the *ΔchvI* growth defect by deletion of *ntrX* (Fig. S6A). We overexpressed (for those genes upregulated by ChvI) or knocked out (for those genes downregulated by ChvI) each of these genes in *ΔchvI* cells and tested their growth capacity in M2X medium.

Only one candidate, *chvT*, had any effect on *ΔchvI* cells. Specifically, deletion of *chvT* partially rescued growth of *ΔchvI* cells in M2X (Fig. 7A and Fig. S6B). Differential regulation of *chvT* expression by ChvI and NtrX may therefore contribute to the growth defect observed in M2X medium.

Discussion

The importance of the C. crescentus ChvGI system for growth in defined medium

To our knowledge, the only previously reported physiological phenotype for *chvGI* mutants in *C. crescentus* is sensitivity to the antibiotic vancomycin (47). However, previous work indicated that ChvGI might be important for growth in defined medium (6). Indeed, deletion of *chvG* or *chvI* caused a distinctive growth defect in M2X medium. *ΔchvI* cultures do grow in M2X upon inoculation from PYE plates, suggesting that the physiologic state of the cell in PYE is initially amenable to growth in defined medium (Fig. 1). However, this tolerance is limited by time, with only higher inocula able to reach high cell density (Fig. 1 and Fig. S2). Why then, can primary overnight cultures persist at high density until back-dilution in fresh M2X? One possibility is that the low pH of M2X at stationary phase preserves *ΔchvI* and *ΔchvG* cells, potentially by triggering phosphorylation of NtrX (Fig. 7B). This model is supported by the observation that *ΔchvI* cells reach higher CFUs when back-diluted in M2X at pH 5.5 vs. pH 6.0 (Fig. S4C). As ~20% of the NtrX pool is phosphorylated in M2G medium at pH 6.0 vs. ~40% at pH 5.5 (by phos-tag analysis), the pH 6–5.5 transition would significantly change the level of unphosphorylated NtrX (48). However, as *ΔchvI* and *ΔchvG* cells also appear to be sensitive to acidic pH, additional factors are likely at play (Fig. S4C). For example, several extracytoplasmic function (ECF) sigma factors are involved in resistance to stationary-phase stress and might play a protective role in *ΔchvI* and *ΔchvG* cells (59-61).

A recent study failed to identify *chvG* or *chvI* as being important for fitness in M2X medium (62). However, in this work M2X cultures were inoculated from PYE starters at high enough density to reach saturation in 5 doublings. Thus, these experiments likely mimicked our primary overnight cultures, obscuring detection of any fitness defects for *chvGI* mutants.

The ChvI transcriptional regulon in C. crescentus

Although ExoR or ChvI transcriptional regulons have been defined in several α-proteobacteria (4, 5, 26, 63), the *C. crescentus* ChvI regulon was unknown prior to this work. We employed RNA-seq to detect direct and indirect transcriptional targets of ChvI in *C. crescentus* (Fig. 6). Our ChvI regulon contained several classes of genes noted in other α-proteobacteria, including those encoding outer membrane proteins and transporters, metabolic enzymes, lipopolysaccharide biosynthesis enzymes, and stress response proteins (4, 5, 26, 63). We note, in particular, that the *C. crescentus* ChvI regulon contained a large number of genes encoding proteins involved in envelope maintenance, including nearly the entire BAM complex, the envelope integrity protein EipA, members of the Tol-Pal complex, and a variety of chaperones and proteases (Fig. 6 and Table S2) (64-67). The idea that ChvGI is

involved in envelope integrity is consistent with previous observations that ChvGI is activated by envelope stress and confers resistance to antibiotics targeting the cell wall (47). However, ~40% of genes regulated by ChvI are annotated generically or as hypotheticals, and thus, more work will be required to characterize the pathways downstream of the ChvGI system. In *A. tumefaciens*, *S. meliloti*, and *C. crescentus*, ChvGI appears to suppress cell motility and/or chemotaxis (5, 15, 20, 26, 68, 69). However, we did not observe transcriptional regulation of any obvious flagellar or chemotaxis genes, suggesting that effects on motility may be due to post-transcriptional regulation and/or alterations in cell-cycle progression (70-72).

Overexpression of the phosphomimetic *chvI(D52E)* allele induced sausage-like cell filamentation in M2X, implicating ChvI in regulating cell division, and cytokinesis in particular. ChvI upregulates several genes related to cell division, including *zauP*, members of the Tol-Pal complex, *smc*, and *nstA* (67, 73-76). We note that overexpression of a proteolytically stable mutant form of *nstA* induces cell filamentation and both *zauP* and the Tol-Pal complex are involved in regulating cytokinesis (73, 76). Perhaps over-induction of these regulon genes, in combination with the cellular state in M2X medium, interferes with proper cell division.

Genetic interactions between ChvGI and NtrYX

The severe growth defect of *ΔchvG* and *ΔchvI* cells in M2X medium allowed us to uncover the first known genetic interaction between *chvGI* and *ntrYX* (Fig. 3). Importantly, deletion of *ntrX* suppressed the growth defect of *ΔchvI* cells, whereas overexpression of non-phosphorylatable *ntrX(D53A)* is deleterious for growth in both *ΔchvI* and WT cells (Fig. 4). These results suggest that the activity of unphosphorylated NtrX is particularly detrimental in cells lacking *chvI*. Therefore, we propose that phosphorylated ChvI and unphosphorylated NtrX oppose each other to regulate growth in defined medium (Fig. 7B). We note that a past study examining connections between ChvI and NtrX in *S. meliloti* did not test whether perturbations in NtrYX signaling might affect *ΔchvI* phenotypes (25). We predict that a similar ChvI–NtrX relationship may be conserved in other α-proteobacteria.

As gain-of-function mutations in *ntrY* suppress the growth defect of *ΔchvI* cells, we also propose that phosphorylation of NtrX relieves its detrimental activity, possibly by changing its transcriptional regulon. Although the global transcriptional effects of NtrX phosphorylation have yet to be characterized, *in vitro* phosphorylation of *Brucella abortus* NtrX does induce conformational changes and alters, but does not weaken, binding to the *ntrYX* promoter (77). Interestingly, we were unable to construct *ΔchvI ΔntrY* and *ΔchvI ΔntrZ* strains, suggesting that these gene deletion combinations are synthetic lethal in PYE medium. As *ntrX* is essential in PYE, the balance between unphosphorylated and phosphorylated NtrX may also be important for growth in rich medium (20).

To identify downstream genes that mediate the oppositional relationship between ChvI and NtrX, we compared their transcriptional regulons (Fig. 6 and Table S1). The ChvI regulon strongly overlapped with that of NtrX, as 80% of the top 30 ChvI-activated

genes are also activated by NtrX (per our >1.5-fold cutoff). By contrast, only 20% of the top 30 NtrX-activated genes exhibit >1.5-fold ChvI-dependence (49). Given that *chvI*, *chvG*, and *hprK* are upregulated by NtrX, it may be the case that NtrX simply activates expression of the *chvIG-hprK* operon, thereby altering transcription of genes in the ChvI regulon (Fig. 7B, grey arrow). Alternatively, loss of NtrX may indirectly suppress ChvGI signaling, in turn affecting expression of the ChvI regulon. Though these scenarios are most consistent with the transcriptome data, it remains formally possible that NtrX independently regulates expression of many of the ChvI regulon genes. Thus, further work is required to determine the exact mechanism by which NtrX regulates expression of genes in the ChvI regulon. The overlap we observed between the ChvI and NtrX regulons may be restricted to *C. crescentus* and close relatives, as *chvG* and *chvI* are not transcriptionally regulated by NtrYX in *Rhodobacter sphaeroides* (40). However, ChvGI and NtrYX may still be transcriptionally linked in more distantly-related α-proteobacterial species, as *ntrX* is part of the *A. tumefaciens* ExoR regulon (26).

The majority of overlapping genes in the ChvI and NtrX regulons cannot account for the detrimental effect of unphosphorylated NtrX on *ΔchvI* cells. Therefore, we focused on eight genes that exhibited opposing transcriptional regulation by ChvI and NtrX (Fig. S6). Only deletion of *chvT* improved the growth of *ΔchvI* cells, indicating that suppression of *chvT* RNA levels by ChvI may be important for growth in M2X medium (Fig. 7). *chvT* is linked to diverse phenotypes in *C. crescentus*, including survival in stationary phase, sensitivity to cell wall-targeting antibiotics, and sensitivity to bacteriocins (47, 78, 79). However, the molecule(s) transported by ChvT remain undefined. High ChvT levels may contribute to defects in transport in defined medium and/or alter membrane integrity, impacting the viability of cells lacking ChvGI (47). It is clear, though, that altered *chvT* expression cannot fully explain the growth deficiency of *ΔchvI* cells in M2X medium. This growth defect may result from the collective action of several genes, and therefore, manipulation of individual candidates may not rescue growth in M2X. Moreover, 15 genes in the ChvI regulon are absent from the NtrX microarray dataset, raising the possibility that one or more may be differentially regulated by ChvI and NtrX (Fig. 6). ChvI and NtrX might also interact more indirectly, as each regulates unique subsets of genes that may affect growth in M2X medium.

On the role of NtrZ

NtrYX is associated with a wide range of physiological responses, from nitrogen metabolism to redox sensing and cell envelope maintenance (25, 35, 39, 40). Despite these phenotypic observations, little is known about the regulation of the NtrY kinase via its periplasmic domain. Our work reveals a new potential activation pathway involving the previously uncharacterized periplasmic protein NtrZ, as well as several key residues in the transmembrane region of NtrY (Fig. 3 and Fig. 7).

ntrZ is one of many genes upregulated by NtrX during log phase growth in M2G medium (49). Our work provides three key findings that support a role for NtrZ in activating NtrY kinase activity or suppressing NtrY phosphatase

activity. First, gain-of-function mutations in both *ntrY* and *ntrZ* can rescue growth of *ΔchvI* cells in M2X medium (Fig. 3 and Fig. 5). In addition, *ΔntrZ*, *ΔntrY*, and *ΔntrY ΔntrZ* cells exhibit lower stationary-phase viability than WT cells (Fig. 5), similar to *ΔntrX* cells (48). Finally, expression of a gain-of-function *ntrY* mutant rescues the *ΔntrZ* stationary-phase phenotype, suggesting that *ntrY* acts downstream of *ntrZ* (Fig. 5). Based on these results, we propose a model in which NtrZ activates NtrY kinase activity (or represses phosphatase activity), promoting NtrX phosphorylation and improving survival during stationary-phase growth in M2X medium (Fig. 7). We acknowledge that our model is based on genetic analyses of *ntrX*, *ntrY*, and *ntrZ* mutants, and thus, will benefit from future experiments that directly assess NtrX phosphorylation. In the future, we are also interested in determining whether NtrZ interacts with the NtrY periplasmic domain or affects NtrY activity indirectly. Several known periplasmic or membrane-bound TCS regulators directly interact with HK periplasmic domains (33, 80-82).

Fernández et al. reported that NtrX phosphorylation is triggered by acidic pH in defined medium (48). Therefore, we hypothesize that activation of NtrY by NtrZ may normally be restricted to acidic pH. Thus, NtrZ and ExoR potentially share a regulatory theme, in which they sense low pH, thereby allowing activation of associated HKs (16, 33, 34). However, it remains to be seen if, as with ExoR, proteolysis plays a role in controlling NtrZ-dependent regulation of NtrY (16). Given the results of our suppressor selection, it would appear that mutations in NtrZ or in the transmembrane helices of NtrY can bypass activation by acidic pH. In an alignment of 100 NtrZ homologs, ranging from 41% to 100% sequence identity, the Y92 position is conserved as an aromatic residue (95% Y) while I99 is conserved as an aliphatic hydrophobic residue (51% I, common L and V substitutions), suggesting that these residues are important for NtrZ function. Further work is required to determine how mutation of Y92 or I99 may alter interaction with the NtrY periplasmic domain or affect a different aspect of NtrZ function. An alignment of the non-cytoplasmic portion of 250 NtrY sequences, ranging from 37% to 100% identity, reveals that the L70 position is largely conserved as an aliphatic hydrophobic residue (94% L) whereas A123 is conserved as a hydrophobic residue (93% A), albeit with occasional bulky-aromatic substitutions. It is unsurprising, then, that the L70H and A123V substitutions appear to affect NtrY function. In fact, several studies have identified transmembrane mutations that alter HK kinase and phosphatase activities (83-85). These results are consistent with observations that signals are transduced from HK periplasmic domains to cytoplasmic domains via changes in the position of transmembrane helices (55, 56).

Unlike the periplasmic kinase regulator ExoR, NtrZ does not contain any conserved domains or protein interaction motifs (86). Moreover, NtrZ appears restricted to the order Caulobacterales, albeit with a few distant homologs in other α-proteobacteria. Notably, neither *B. abortus*, *S. meliloti*, nor *A. tumefaciens* contain NtrZ homologs, and conservation of the non-cytoplasmic region of NtrY is quite low between *C. crescentus* and these organisms (24–27% identity). However, L70 is largely conserved (L or V) and A123 is entirely conserved between these NtrY

homologs. Thus, the L70H and A123V substitutions may have similar effects on NtrY activity in these organisms, and further analyses of these mutants may shed light on a conserved NtrY activation mechanism. It will also be interesting to see if *S. meliloti*, *A. tumefaciens*, and *B. abortus*, like *C. crescentus,* employ periplasmic NtrY regulators.

Materials and Methods

Strains and Plasmids

All plasmids were constructed using standard molecular biology techniques. See Table S2 for strain, plasmid, and primer information. Plasmids for generating in-frame deletions were generated by cloning homologous upstream and downstream regions into pNPTS138. Transcriptional reporter plasmids were generated by cloning 400–500 bp upstream of the open reading frame into pRKlac290. For overexpression strains, ORFs were inserted into pMT585, a plasmid for xylose-inducible expression that integrates at the *xylX* locus. Plasmids were transformed into *C. crescentus* CB15 strain by electroporation or tri-parental mating. In-frame deletion and allele-replacement strains were generated by a double recombination strategy involving *sacB* counterselection on PYE plates supplemented with 3% sucrose (87). For *ΔntrX* knockout strains, counterselection was carried out on M2X + 0.5% sucrose plates. *ΔntrX* and *ΔchvI ΔntrX* strains were grown only on M2 medium. All *C. crescentus* strains were grown at 30°C. For strains carrying pRKlac290 plasmids, oxytetracycline was added to 1 μg/mL in liquid and 2 μg/mL in PYE agar or 1 μg/mL in M2X agar.

Measurement of Growth in M2X Medium

Primary M2X cultures were inoculated from plates to an approximate density of OD_{660} 0.02-0.10 and grown overnight. Overnight cultures were back-diluted to OD_{660} = 0.025 and OD_{660} was recorded at the indicated times. To enumerate colony forming units, samples were taken at the indicated time points and 10-fold serial dilutions were plated on PYE agar. For pH experiments, M2X medium was adjusted to the indicated pH using HCl.

For experiments with controlled starting densities, cells were resuspended in M2X medium directly from PYE plates. These resuspensions were then diluted to the indicated OD_{660} and the cultures were titered for CFUs. In washing experiments, 1 mL resuspended cells were spun down at 8k × *g* for 3 min and resuspended in 1 mL fresh M2X medium once (1X) or twice (2X) before dilution. Plotting and statistical analyses were carried out using Prism (Graphpad).

Microscopy

Samples of *ΔchvG* and *ΔchvI* cells were taken from overnight M2X or PYE + 0.15% xylose cultures and imaged with a DMI6000B (Leica) microscope in phase contrast using a HC PL APO 63x/1.4na oil Ph3 CS2 objective. Images were captured using an Orca-R^2 C10600 digital camera (Hamamatsu) controlled by Leica Application Suite X (Leica). Images were processed using Fiji (88, 89).

Suppressor Screen

Overnight M2X cultures of *ΔchvG* and *ΔchvI* cells were back-diluted to OD_{660} = 0.025 in M2X medium. Cultures initially saturated at OD_{660} ~0.1 before growing to higher density (OD_{660} = 0.5–0.8) after 2-3 days growth. From each culture, single colonies were isolated on PYE plates. Isolated strains were then tested for suppression by M2X growth curves. The origin of each suppressor strain is as follows: culture 1 (*ΔIS1*), culture 2 (*ΔIS2, ΔIS3*), culture 3 (*ΔGS1*), culture 4 (*ΔGS2, ΔGS3*). Genomic DNA was isolated from 1 mL of overnight culture grown in PYE medium, using guanidinium thiocyanate (90). Sequencing was performed by the Microbial Genome Sequencing Center (Pittsburgh, PA) using a single library preparation method based upon the Illumina Nextera Kit. Sequences were aligned to the *C. crescentus* NA1000 reference genome (GenBank accession number CP001340) using breseq (91).

Transcriptome Deep Sequencing (RNA-seq)

2 mL of PYE medium was inoculated with *ΔchvI* EV (*ΔchvI xylX*::pMT585) and *ΔchvI chvI(D52E)++* (*ΔchvI xylX*::pMT585-*chvI(D52E)*) cells and grown overnight. Cultures were diluted to OD_{660} = 0.001 in 2 mL fresh PYE and grown for 22.5 h. Cultures were diluted to OD_{660} = 0.075 in 5 mL PYE + 0.15% xylose and grown for 3.5 h before TRIzol extraction and RNA isolation, as described

previously (92). RNA-seq libraries were prepared using an Illumina TruSeq stranded RNA kit and sequenced on an Illumina NextSEQ500 instrument at the University of Chicago Functional Genomics Facility. Sequencing data were analyzed using CLC Genomics Workbench 20 (Qiagen) by mapping reads to the *C. crescentus* NA1000 genome (78). Motif searching was carried out using MEME (93). Heatmaps were generated using Java Treeview3 and hypergeometric analysis was performed using phyper in R (94, 95).

β-galactosidase Assays

For assays of WT vs. *ΔchvI* strains, cells were grown overnight in 2 mL PYE medium. Then, 500 μL of each culture was centrifuged at 8k × *g* for 3 min and resuspended in 500 μL M2X medium. Resuspended cultures were used to inoculate 2 mL M2X medium at a starting OD_{660} of 0.075. Cultures were grown for 4 h before assaying β-galactosidase activity. For assays of WT vs. *ΔntrX* strains, cells were grown overnight in 2 mL M2X medium. Overnight cultures were diluted in M2X medium such that they would reach OD_{660} = 0.1–0.2 after 23.5 h of growth. β-galactosidase assays were performed as previously described using 200 μL of M2X culture + 100 μL sterile PYE medium as an emulsifier (96). Plotting and statistical analyses were carried out using Prism (Graphpad).

Accession Number(s)

RNA-seq data are available in the NCBI GEO database under accession number GSE168965.

Acknowledgements

We thank Clare Kirkpatrick, Régis Hallez, Alex Quintero, and members of the Crosson laboratory for helpful discussion, and Jen Mach and Plant Editors for constructive feedback on the manuscript. Research in this publication was supported by the National Institute of General Medical Sciences of the National Institutes of Health (NIH) under Award Numbers F32 GM128283 (B.J.S.) and R35 GM131762 (S.C.). The content is solely the responsibility of the authors and does not necessarily represent the official views of the National Institutes of Health.

The authors declare no conflict of interest.

References

1. Stock AM, Robinson VL, Goudreau PN. 2000. Two-Component Signal Transduction. Annu Rev Biochem 69:183–215.
2. Crosson S, McGrath PT, Stephens C, McAdams HH, Shapiro L. 2005. Conserved modular design of an oxygen sensory/signaling network with species-specific output. Proc Natl Acad Sci U S A 102:8018–8023.
3. David M, Daveran ML, Batut J, Dedieu A, Domergue O, Ghai J, Hertig C, Boistard P, Kahn D. 1988. Cascade Regulation of *nif* Gene Expression in *Rhizobium meliloti*. Cell 54:671–683.
4. Viadas C, Rodríguez MC, Sangari FJ, Gorvel JP, García-Lobo JM, López-Goñi I. 2010. Transcriptome Analysis of the *Brucella abortus* BvrR/BvrS Two-Component Regulatory System. PLoS ONE 5:e10216.
5. Ratib NR, Sabio EY, Mendoza C, Barnett MJ, Clover SB, Ortega JA, Cruz Dela FM, Balderas D, White H, Long SR, Chen EJ. 2018. Genome-wide identification of genes directly regulated by ChvI and a consensus sequence for ChvI binding in *Sinorhizobium meliloti*. Mol Microbiol 110:596–615.
6. Fröhlich KS, Förstner KU, Gitai Z. 2018. Post-transcriptional gene regulation by an Hfq-independent small RNA in *Caulobacter crescentus*. Nucleic Acids Res 66:325.
7. Landa AS, Cerdá JP, Grilló MJ, Moreno E, Moriyón I, Blasco JM, Gorvel JP, Goñi IL. 1998. A two-component regulatory system playing a critical role in plant pathogens and endosymbionts is present in *Brucella abortus* and controls cell invasion and virulence. Mol Microbiol 29:125–138.
8. Charles TC, Nester EW. 1993. A chromosomally encoded two-component sensory transduction system is required for virulence of *Agrobacterium tumefaciens*. J Bacteriol 175:6614–6625.
9. Gottschlich L, Geiser P, Bortfeld-Miller M, Field CM, Vorholt JA. 2019. Complex general stress response regulation in *Sphingomonas melonis* Fr1 revealed by transcriptional analyses. Sci Rep 9:9404.
10. Kaczmarczyk A, Hochstrasser R, Vorholt JA, Francez-Charlot A. 2014. Complex two-component signaling regulates the general stress

response in Alphaproteobacteria. Proc Natl Acad Sci U S A 111:E5196–204.
11. Lori C, Kaczmarczyk A, de Jong I, Jenal U. 2018. A Single-Domain Response Regulator Functions as an Integrating Hub To Coordinate General Stress Response and Development in Alphaproteobacteria. mBio 9:e00809–18.
12. Francis VI, Porter SL. 2019. Multikinase Networks: Two-Component Signaling Networks Integrating Multiple Stimuli. Annu Rev Microbiol 73:199–223.
13. Howell A, Dubrac S, Noone D, Varughese KI, Devine K. 2006. Interactions between the YycFG and PhoPR two-component systems in *Bacillus subtilis*: the PhoR kinase phosphorylates the non-cognate YycF response regulator upon phosphate limitation. Mol Microbiol 59:1199–1215.
14. Perego M, Hanstein C, Welsh KM, Djavakhishvili T, Glaser P, Hoch JA. 1994. Multiple Protein-Aspartate Phosphatases Provide a Mechanism for the Integration of Diverse Signals in the Control of Development in *B. subtilis*. Cell 79:1047–1055.
15. Wells DH, Chen EJ, Fisher RF, Long SR. 2007. ExoR is genetically coupled to the ExoS-ChvI two-component system and located in the periplasm of *Sinorhizobium meliloti*. Mol Microbiol 64:647–664.
16. Lu H-Y, Luo L, Yang M-H, Cheng H-P. 2012. *Sinorhizobium meliloti* ExoR Is the Target of Periplasmic Proteolysis. J Bacteriol 194:4029–4040.
17. Stein BJ, Fiebig A, Crosson S. 2020. Feedback Control of a Two-Component Signaling System by an Fe-S-Binding Receiver Domain. mBio 11:183.
18. Noriega CE, Lin H-Y, Chen L-L, Williams SB, Stewart V. 2010. Asymmetric cross-regulation between the nitrate-responsive NarX-NarL and NarQ-NarP two-component regulatory systems from *Escherichia coli* K-12. Mol Microbiol 75:394–412.
19. Miller MB, Skorupski K, Lenz DH, Taylor RK, Bassler BL. 2002. Parallel quorum sensing systems converge to regulate virulence in *Vibrio cholerae*. Cell 110:303–314.
20. Skerker JM, Prasol MS, Perchuk BS, Biondi EG, Laub MT. 2005. Two-Component Signal Transduction Pathways Regulating Growth and Cell Cycle Progression in a Bacterium: A System-Level Analysis. PLoS Biol 3:e334.
21. Bijlsma JJE, Groisman EA. 2003. Making informed decisions: regulatory interactions between two-component systems. Trends Microbiol 11:359–366.
22. Birkey SM, Liu W, Zhang X, Duggan MF, Hulett FM. 1998. Pho signal transduction network reveals direct transcriptional regulation of one two-component system by another two-component regulator: *Bacillus subtilis* PhoP directly regulates production of ResD. Mol Microbiol 30:943–953.
23. Mouslim C, Groisman EA. 2003. Control of the *Salmonella ugd* gene by three two-component regulatory systems. Mol Microbiol 47:335–344.
24. Huang J, Carney BF, Denny TP, Weissinger AK, Schell MA. 1995. A complex network regulates expression of eps and other virulence genes of *Pseudomonas solanacearum*. J Bacteriol 177:1259–1267.
25. Wang D, Xue H, Wang Y, Yin R, Xie F, Luo L. 2013. The *Sinorhizobium meliloti ntrX* Gene Is Involved in Succinoglycan Production, Motility, and Symbiotic Nodulation on Alfalfa. Appl Environ Microbiol 79:7150–7159.
26. Heckel BC, Tomlinson AD, Morton ER, Choi JH, Fuqua C. 2014. *Agrobacterium tumefaciens* ExoR Controls Acid Response Genes and Impacts Exopolysaccharide Synthesis, Horizontal Gene Transfer, and Virulence Gene Expression. J Bacteriol 196:3221–3233.
27. Mantis NJ, Winans SC. 1993. The chromosomal response regulatory gene *chvI* of *Agrobacterium tumefaciens* complements an *Escherichia coli phoB* mutation and is required for virulence. J Bacteriol 175:6626–6636.
28. Cheng HP, Walker GC. 1998. Succinoglycan production by *Rhizobium meliloti* is regulated through the ExoS-ChvI two-component regulatory system. J Bacteriol 180:20–26.
29. Guzman-Verri C, Manterola L, Sola-Landa A, Parra A, Cloeckaert A, Garin J, Gorvel JP, Moriyon I, Moreno E, Lopez-Goni I. 2002. The two-component system BvrR/BvrS essential for *Brucella abortus* virulence regulates the expression of outer membrane proteins with counterparts in members of the *Rhizobiaceae*. Proc Natl Acad Sci U S A 99:12375–12380.
30. Yao SY, Luo L, Har KJ, Becker A, Ruberg S, Yu GQ, Zhu JB, Cheng HP. 2004. *Sinorhizobium meliloti* ExoR and ExoS Proteins Regulate both Succinoglycan and Flagellum Production. J Bacteriol 186:6042–6049.
31. Foreman DL, Vanderlinde EM, Bay DC, Yost CK. 2010. Characterization of a Gene Family of Outer Membrane Proteins (*ropB*) in *Rhizobium leguminosarum* bv. *viciae* VF39SM and the Role of the Sensor Kinase ChvG in Their Regulation. J Bacteriol 192:975–983.
32. Quebatte M, Dehio M, Tropel D, Basler A, Toller I, Raddatz G, Engel P, Huser S, Schein H, Lindroos

HL, Andersson SGE, Dehio C. 2010. The BatR/BatS Two-Component Regulatory System Controls the Adaptive Response of *Bartonella henselae* during Human Endothelial Cell Infection. J Bacteriol 192:3352–3367.
33. Chen EJ, Sabio EA, Long SR. 2008. The periplasmic regulator ExoR inhibits ExoS/ChvI two-component signalling in *Sinorhizobium meliloti*. Mol Microbiol 69:1290–1303.
34. Wu C-F, Lin J-S, Shaw G-C, Lai E-M. 2012. Acid-Induced Type VI Secretion System Is Regulated by ExoR-ChvG/ChvI Signaling Cascade in *Agrobacterium tumefaciens*. PLOS Pathog 8:e1002938.
35. Pawlowski K, Klosse U, de Bruijn FJ. 1991. Characterization of a novel *Azorhizobium caulinodans* ORS571 two-component regulatory system, NtrY/NtrX, involved in nitrogen fixation and metabolism. Molec Gen Genet 231:124–138.
36. Ishida ML, Assumpção MC, Machado HB, Benelli EM, Souza EM, Pedrosa FO. 2002. Identification and characterization of the two-component NtrY/NtrX regulatory system in *Azospirillum brasilense*. Braz J Med Biol Res 35:651–661.
37. Cheng Z, Lin M, Rikihisa Y. 2014. *Ehrlichia chaffeensis* Proliferation Begins with NtrY/NtrX and PutA/GlnA Upregulation and CtrA Degradation Induced by Proline and Glutamine Uptake. mBio 5:1.
38. Atack JM, Srikhanta YN, Djoko KY, Welch JP, Hasri NHM, Steichen CT, Hoven RNV, Grimmond SM, Othman DSMP, Kappler U, Apicella MA, Jennings MP, Edwards JL, McEwan AG. 2013. Characterization of an *ntrX* Mutant of *Neisseria gonorrhoeae* Reveals a Response Regulator That Controls Expression of Respiratory Enzymes in Oxidase-Positive Proteobacteria. J Bacteriol 195:2632–2641.
39. del Carmen Carrica M, Fernández I, Martí MA, Paris G, Goldbaum FA. 2012. The NtrY/X two-component system of *Brucella* spp. acts as a redox sensor and regulates the expression of nitrogen respiration enzymes. Mol Microbiol 85:39–50.
40. Lemmer KC, Alberge F, Myers KS, Dohnalkova AC, Schaub RE, Lenz JD, Imam S, Dillard JP, Noguera DR, Donohue TJ. 2020. The NtrYX Two-Component System Regulates the Bacterial Cell Envelope. mBio 11:a000414.
41. Calatrava-Morales N, Nogales J, Ameztoy K, van Steenbergen B, Soto MJ. 2017. The NtrY/NtrX System of *Sinorhizobium meliloti* GR4 Regulates Motility, EPS I Production, and Nitrogen Metabolism but Is Dispensable for Symbiotic Nitrogen Fixation. MPMI 30:566–577.
42. Bonato P, Alves LR, Osaki JH, Rigo LU, Pedrosa FO, Souza EM, Zhang N, Schumacher J, Buck M, Wassem R, Chubatsu LS. 2016. The NtrY–NtrX two-component system is involved in controlling nitrate assimilation in *Herbaspirillum seropedicae* strain SmR1. FEBS J 283:3919–3930.
43. Urtecho G, Campbell DE, Hershey DM, Hussain FA, Whitaker RJ, O'Toole GA. 2020. Discovering the Molecular Determinants of *Phaeobacter inhibens* Susceptibility to Phaeobacter Phage MD18. mSphere 5:666.
44. Drepper T, Wiethaus J, Giaourakis D, GroÃ S, Schubert B, Vogt M, Wiencek Y, McEwan AG, Masepohl B. 2006. Cross-talk towards the response regulator NtrC controlling nitrogen metabolism in *Rhodobacter capsulatus*. FEMS Microbiol Lett 258:250–256.
45. Poindexter JS. 1964. Biological properties and classification of the *Caulobacter* group. Bacteriol Rev 28:231–295.
46. Wilhelm RC. 2018. Following the terrestrial tracks of *Caulobacter* - redefining the ecology of a reputed aquatic oligotroph. ISME J 12:3025–3037.
47. Vallet S-U, Hansen LH, Bistrup FC, Laursen SA, Chapalay JB, Chambon M, Turcatti G, Viollier PH, Kirkpatrick CL. 2020. Loss of Bacterial Cell Pole Stabilization in *Caulobacter crescentus* Sensitizes to Outer Membrane Stress and Peptidoglycan-Directed Antibiotics. mBio 11:13.
48. Fernández I, Sycz G, Goldbaum FA, del Carmen Carrica M. 2018. Acidic pH triggers the phosphorylation of the response regulator NtrX in alphaproteobacteria. PLoS ONE 13:e0194486.
49. Capra EJ, Perchuk BS, Skerker JM, Laub MT. 2012. Adaptive Mutations that Prevent Crosstalk Enable the Expansion of Paralogous Signaling Protein Families. Cell 150:222–232.
50. Karl KE, David WS, Sydney K. 1993. Glutamate at the site of phosphorylation of nitrogen-regulatory protein NTRC mimics aspartyl-phosphate and activates the protein. J Mol Bio 232:67–78.
51. Moore JB, Shiau SP, Reitzer LJ. 1993. Alterations of highly conserved residues in the regulatory domain of nitrogen regulator I (NtrC) of *Escherichia coli*. J Bacteriol 175:2692–2701.
52. Gupte G, Woodward C, Stout V. 1997. Isolation and characterization of *rcsB* mutations that affect colanic acid capsule synthesis in *Escherichia coli* K-12. J Bacteriol 179:4328–4335.
53. Lan CY, Igo MM. 1998. Differential expression of the OmpF and OmpC porin proteins in *Escherichia*

coli K-12 depends upon the level of active OmpR. J Bacteriol 180:171–174.
54. Gushchin I, Gordeliy V. 2018. Transmembrane Signal Transduction in Two-Component Systems: Piston, Scissoring, or Helical Rotation? Bioessays 40:1700197.
55. Gushchin I, Melnikov I, Polovinkin V, Ishchenko A, Yuzhakova A, Buslaev P, Bourenkov G, Grudinin S, Round E, Balandin T, Borshchevskiy V, Willbold D, Leonard G, Büldt G, Popov A, Gordeliy V. 2017. Mechanism of transmembrane signaling by sensor histidine kinases. Science 356:eaah6345.
56. Molnar KS, Bonomi M, Pellarin R, Clinthorne GD, Gonzalez G, Goldberg SD, Goulian M, Sali A, DeGrado WF. 2014. Cys-Scanning Disulfide Crosslinking and Bayesian Modeling Probe the Transmembrane Signaling Mechanism of the Histidine Kinase, PhoQ. Structure 22:1239–1251.
57. Skerker JM, Perchuk BS, Siryaporn A, Lubin EA, Ashenberg O, Goulian M, Laub MT. 2008. Rewiring the Specificity of Two-Component Signal Transduction Systems. Cell 133:1043–1054.
58. Yamada S, Sugimoto H, Kobayashi M, Ohno A, Nakamura H, Shiro Y. 2009. Structure of PAS-Linked Histidine Kinase and the Response Regulator Complex. Structure 17:1333–1344.
59. Lourenço RF, Kohler C, Gomes SL. 2011. A two-component system, an anti-sigma factor and two paralogous ECF sigma factors are involved in the control of general stress response in *Caulobacter crescentus*. Mol Microbiol 80:1598–1612.
60. Alvarez-Martinez CE, Lourenço RF, Baldini RL, Laub MT, Gomes SL. 2007. The ECF sigma factor σ Tis involved in osmotic and oxidative stress responses in *Caulobacter crescentus*. Mol Microbiol 66:1240–1255.
61. Alvarez-Martinez CE, Baldini RL, Gomes SL. 2006. A *Caulobacter crescentus* Extracytoplasmic Function Sigma Factor Mediating the Response to Oxidative Stress in Stationary Phase. J Bacteriol 188:1835–1846.
62. Hentchel KL, Ruiz LMR, Curtis PD, Fiebig A, Coleman ML, Crosson S. 2019. Genome-scale fitness profile of *Caulobacter crescentus* grown in natural freshwater. ISME J 13:523–536.
63. Chen EJ, Fisher RF, Perovich VM, Sabio EA, Long SR. 2009. Identification of Direct Transcriptional Target Genes of ExoS/ChvI Two-Component Signaling in *Sinorhizobium meliloti*. J Bacteriol 191:6833–6842.
64. Herrou J, Willett JW, Fiebig A, Varesio LM, Czyż DM, Cheng JX, Ultee E, Briegel A, Bigelow L, Babnigg G, Kim Y, Crosson S. 2019. Periplasmic protein EipA determines envelope stress resistance and virulence in *Brucella abortus*. Mol Microbiol 111:637–661.
65. Hagan CL, Silhavy TJ, Kahne D. 2011. β-Barrel Membrane Protein Assembly by the Bam Complex. Annu Rev Biochem 80:189-210.
66. Anwari K, Poggio S, Perry A, Gatsos X, Ramarathinam SH, Williamson NA, Noinaj N, Buchanan S, Gabriel K, Purcell AW, Jacobs-Wagner C, Lithgow T. 2010. A modular BAM complex in the outer membrane of the alpha-proteobacterium *Caulobacter crescentus*. PLoS ONE 5:e8619.
67. Yeh Y-C, Comolli LR, Downing KH, Shapiro L, McAdams HH. 2010. The *Caulobacter* Tol-Pal complex is essential for outer membrane integrity and the positioning of a polar localization factor. J Bacteriol 192:4847–4858.
68. Wang C, Kemp J, Da Fonseca IO, Equi RC, Sheng X, Charles TC, Sobral BWS. 2010. *Sinorhizobium meliloti* 1021 Loss-of-Function Deletion Mutation in *chvI* and Its Phenotypic Characteristics. MPMI 23:153–160.
69. Tomlinson AD, Ramey-Hartung B, Day TW, Merritt PM, Fuqua C. 2010. *Agrobacterium tumefaciens* ExoR represses succinoglycan biosynthesis and is required for biofilm formation and motility. Microbiology 156:2670–2681.
70. Aldridge P, Jenal U. 1999. Cell cycle-dependent degradation of a flagellar motor component requires a novel-type response regulator. Mol Microbiol 32:379–391.
71. Hershey DM, Fiebig A, Crosson S. 2021. Flagellar Perturbations Activate Adhesion through Two Distinct Pathways in *Caulobacter crescentus*. mBio 12.
72. Ardissone S, Viollier PH. 2015. Interplay between flagellation and cell cycle control in *Caulobacter*. Curr Opin Microbiol 28:83–92.
73. Woldemeskel SA, McQuillen R, Hessel AM, Xiao J, Goley ED. 2017. A conserved coiled-coil protein pair focuses the cytokinetic Z-ring in *Caulobacter crescentus*. Mol Microbiol 105:721–740.
74. Schwartz MA, Shapiro L. 2011. An SMC ATPase mutant disrupts chromosome segregation in *Caulobacter*. Mol Microbiol 82:1359–1374.
75. Jensen RB, Shapiro L. 1999. The *Caulobacter crescentus smc* gene is required for cell cycle progression and chromosome segregation. Proc Natl Acad Sci U S A 96:10661–10666.
76. Narayanan S, Janakiraman B, Kumar L, Radhakrishnan SK. 2015. A cell cycle-controlled

redox switch regulates the topoisomerase IV activity. Genes Dev 29:1175–1187.
77. Fernández I, Cornaciu I, Carrica MDC, Uchikawa E, Hoffmann G, Sieira R, Márquez JA, Goldbaum FA. 2017. Three-Dimensional Structure of Full-Length NtrX, an Unusual Member of the NtrC Family of Response Regulators. J Mol Bio 429:1192–1212.
78. Marks ME, Castro-Rojas CM, Teiling C, Du L, Kapatral V, Walunas TL, Crosson S. 2010. The Genetic Basis of Laboratory Adaptation in *Caulobacter crescentus*. J Bacteriol 192:3678–3688.
79. García-Bayona L, Gozzi K, Laub MT. 2019. Mechanisms of Resistance to the Contact-Dependent Bacteriocin CdzC/D in *Caulobacter crescentus*. J Bacteriol 201.
80. Hu X, Zhao J, DeGrado WF, Binns AN. 2013. *Agrobacterium tumefaciens* recognizes its host environment using ChvE to bind diverse plant sugars as virulence signals. Proc Natl Acad Sci U S A 110:678–683.
81. Göpel Y, Görke B. 2018. Interaction of lipoprotein QseG with sensor kinase QseE in the periplasm controls the phosphorylation state of the two-component system QseE/QseF in *Escherichia coli*. PLOS Genet 14:e1007547.
82. Lippa AM, Goulian M. 2009. Feedback Inhibition in the PhoQ/PhoP Signaling System by a Membrane Peptide. PLOS Genet 5:e1000788.
83. Hsing W, Russo FD, Bernd KK, Silhavy TJ. 1998. Mutations that alter the kinase and phosphatase activities of the two-component sensor EnvZ. J Bacteriol 180:4538–4546.
84. Lemmin T, Soto CS, Clinthorne G, DeGrado WF, Peraro MD. 2013. Assembly of the Transmembrane Domain of *E. coli* PhoQ Histidine Kinase: Implications for Signal Transduction from Molecular Simulations. PLOS Comput Biol 9:e1002878.
85. Goldberg SD, Clinthorne GD, Goulian M, DeGrado WF. 2010. Transmembrane polar interactions are required for signaling in the *Escherichia coli* sensor kinase PhoQ. PNAS 107:8141–8146.
86. Wiech EM, Cheng H-P, Singh SM. 2015. Molecular modeling and computational analyses suggests that the *Sinorhizobium meliloti* periplasmic regulator protein ExoR adopts a superhelical fold and is controlled by a unique mechanism of proteolysis. Protein Sci 24:319–327.
87. Ried JL, Collmer A. 1987. An *nptI-sacB-sacR* cartridge for constructing directed, unmarked mutations in Gram-negative bacteria by marker exchange-eviction mutagenesis. Gene 57:239–246.
88. Schindelin J, Arganda-Carreras I, Frise E, Kaynig V, Longair M, Pietzsch T, Preibisch S, Rueden C, Saalfeld S, Schmid B, Tinevez J-Y, White DJ, Hartenstein V, Eliceiri K, Tomancak P, Cardona A. 2012. Fiji: an open-source platform for biological-image analysis. Nat Meth 9:676–682.
89. Schneider CA, Rasband WS, Eliceiri KW. 2012. NIH Image to ImageJ: 25 years of image analysis. Nat Meth 9:671–675.
90. Pitcher DG, Saunders NA, Owen RJ. 1989. Rapid extraction of bacterial genomic DNA with guanidium thiocyanate. Lett Appl Microbiol 8:151–156.
91. Daniel E Deatherage JEB. 2014. Identification of mutations in laboratory evolved microbes from next-generation sequencing data using *breseq*. Methods Mol Biol 1151:165–188.
92. Tien MZ, Stein BJ, Crosson S, Silhavy TJ. 2018. Coherent Feedforward Regulation of Gene Expression by *Caulobacter* σT and GsrN during Hyperosmotic Stress. J Bacteriol 200:47.
93. Bailey TL, Boden M, Buske FA, Frith M, Grant CE, Clementi L, Ren J, Li WW, Noble WS. 2009. MEME SUITE: tools for motif discovery and searching. Nucleic Acids Res 37:W202–W208.
94. Saldanha AJ. 2004. Java Treeview—extensible visualization of microarray data. Bioinformatics 20:3246–3248.
95. R Core Team. 2020. R: A language and environment for statistical computing. R Foundation for Statistical Computing, Vienna, Austria. https://wwwR-project.org/
96. Foreman R, Fiebig A, Crosson S. 2012. The LovK-LovR Two-Component System Is a Regulator of the General Stress Pathway in *Caulobacter crescentus*. J Bacteriol 194:3038–3049.
97. Zhou B, Schrader JM, Kalogeraki VS, Abeliuk E, Dinh CB, Pham JQ, Cui ZZ, Dill DL, McAdams HH, Shapiro L. 2015. The Global Regulatory Architecture of Transcription during the *Caulobacter* Cell Cycle. PLOS Genet 11:e1004831.